Formation of the Quasi-stationary Baiu Front to the South of the Japan Islands in Early May of 1979

By Kuranoshin Kato

Water Research Institute of Nagoya University, Nagoya 464-01, Japan

and

Yasumasa Kodama

Department of Earth Science, Faculty of Science, Hirosaki University, Hirosaki 036, Japan
(Manuscript received 29 July 1991, in revised form 13 December 1991)

Abstract

The formation of the "quasi-stationary" Baiu front at the beginning of May 1979 and its relation to the seasonal transition of the large-scale baroclinicity in East Asia was examined by using the observational data.

The frontal zone to the south of the Japan Islands, corresponding to the southern branch of the middle-level westerly jet around the Tibetan Plaeau, is characterized by the alternative passages of synoptic-scale extratropical cyclones and anticyclones in April. On the other hand, the cloud belt associated with the stationary front is sustained at ~25°N in May, even after the passage of the synoptic-scale (or larger meso-α-scale) cyclone at ~30°N. In other words, the frontal zone there becomes quasi-stationary at the beginning of May (the formation of the "quasi-stationary Baiu front" around Japan). The analysis of the location of the front on twice-daily surface weather maps in 1985, 1986, 1987 and 1988, as well as 1979, shows that the change into the quasi-stationary frontal zone occurred in early May of those other years.

The two baroclinic zones, corresponding to the southern and the northern branches of the westerly jet, respectively, are separate from each other around the Japan Islands in May. This results in the weakening of baroclinicity in May just to the north of the Baiu front as well as across the Baiu front. Thus the development of a migratory anticyclone is suppressed, which provides a favorable condition for sustaining the "quasi-stationary" Baiu front in May.

It is noted that the change into the "quasi-stationary" frontal zone at the beginning of May 1979 mentioned above is a different event from the abrupt disappearance of the temperature gradient across the Baiu front in China in late May pointed out by Kato (1985a, 1987).

1. Introduction

The Baiu front corresponding to the northern boundary of the maritime tropical air mass (or monsoon air mass) appears throughout early summer and is characterized by a large horizontal moisture gradient. The Baiu front is the significant subtropical front, and the huge northward flux of moisture from the subtropical high area sustains the rainfall activity of the front. Another interesting feature of the Baiu front is the quasi-stationary belt-shaped cloud zone extending from west to east, while the polar front, as in East Siberia in the warmer season, is characterized by the alternative passages of synoptic-scale cyclones and anticyclones (Akiyama, 1973; Saito, 1966; Ninomiya, 1984, 1989; Ninomiya and Muraki, 1986; Kato, 1985a, 1987, 1989).

Kato (1985b) pointed out that, based on some examples of the GMS images for each stage of the seasonal transition during early summer of 1979, the belt-shaped cloud zone is sustained during a few days after the passage of a synoptic-scale or meso-α-scale cloud area. However, he did not examine the large-scale atmospheric processes which characterize the quasi-stationary cloud zone.

As for the seasonal evolution of the characteristics of the Baiu front, many studies have been made. The Baiu (Mei-yu) front extends from South China to the south of the Japan Islands (~25°N) by May (Gao and Xu, 1962; Yoshino, 1965, 1966), and the horizontal temperature gradient in the lower layer

there is not small (Stage A in Kato (1989) or "Pre-Baiu" in Ninomiya and Muraki (1986)). The temperature gradient around the Baiu front in South China vanishes abruptly in late May. However, the temperature gradient is sustained throughout early summer around Japan (Ninomiya and Muraki, 1986). At that time the Baiu trough extending from the Bering Sea (~60°N/170°E) to North China (~35°N/115°E) is formed just to the north of the front, corresponding to the path of a slow-moving upper-level cut-off low (Stage B or "Early-Baiu") (Ninomiya and Muraki, 1986; Ninomiya, 1989; Saito, 1985).

In the middle of June the Baiu front moves northward to Central China (~30°N) (Gao and Xu, 1962; Yoshino, 1965, 1966; Yu, 1980; Tao and Ding, 1981). The anticyclonic circulation with a strong low-level southerly wind around South China is enhanced due to the establishment of the Northern Summer Monsoon (Indian Monsoon) circulation (Stage C or "Peak-Baiu") (Kato, 1989; Matsumoto, 1984; Ninomiya, 1989; Ninomiya and Muraki, 1986; Tao *et al.*, 1983).

According to climatological studies, the frontal zone, defined as the zone with the maximum appearance frequency of a front on daily weather maps at the surface level (or that with the maximum of mean cloud amount), is located from South China to the south of Japan from February to May (Yoshimura, 1967; Nitta, 1986; Kodama and Asai, 1988; Yamakawa, 1984). However, it has not yet been clarified when and how the frontal zone becomes "quasi-stationary" during the seasonal march.

Murakami and Huang (1984) pointed out an important effect of the frequent initiation of meso-α-scale disturbances (~1000 km in diameter) around the Tibetan Plateau on the rainfall activity on the Baiu front in China, although the characteristics of the disturbances are very different before and after the onset of the Indian Monsoon. On the other hand, Yamakawa (1988) demonstrated that a "migratory anticyclone-type pressure pattern", in which the front is not indicated on daily surface weather maps around Japan, appears frequently in spring. Thus it would be useful to examine the evolution of the cloud area and the behavior of anticyclones (which could interrupt the persistence of the cloud zone) after the passages of the disturbances, in order to understand the process associated with the quasi-stationary character of the front. Since the alternative passages of synoptic-scale cyclones and anticyclones (wavelength of a few 1000 km) is caused by the baroclinic instability, we will present a discussion in relation to the seasonal transition of baroclinicity around the frontal zone.

In the present study we will examine the large-scale circulations and the cloud distributions around the frontal zone in East Asia based on the observational data during early summer of 1979. Since the "change" into the "quasi-stationary" character was observed clearly around the Japan Islands (to the east of ~125°E) in early May, the variations of the cloud amounts there will be mainly examined (as for the frontal zone in China, the cloud area tends to persist also in April, according to the figure presenting the time-latitude sections of GMS visual pictures at 06 GMT at 115°E and 135°E in early summer of 1979 by Kato (1985a)). Although the characteristics of the large-scale circulations are very different and the dominant processes sustaining the "quasi-stationary" front might be rather different among the stages in the seasonal march, we will focus our attention to the front in May (Stage A) by comparison with the situation in April.

2. Data sources

In order to examine the temporal variation of cloud amount, we will use the Infra Red observation data (IR) obtained by the GMS-1 geostationary satellite. Murakami (1983) has edited 3-hourly IR observations (about 5 km in spatial resolution) to yield the data set of the index of deep cumulus convection, I_C. He has compiled T_{BB} (equivalent blackbody temperature) values for every 1° longitude/latitude square mesh in the form of a temperature histogram (at intervals of 10 K) along with their mean value and standard deviation within the mesh.

In the present study, the cloud amount is defined as the ratio of the number of cloud pixels to the total number of pixels within the 1°×1° mesh. We evaluate the amounts (in tenth) of the cloud whose top is higher than the 700 mb level (which is referred to as CA7 hereafter) and that whose top is higher than the 400 mb level (referred to as CA4) by utilizing the every 3-hourly IR histogram data provided by Murakami (1983) and the three-dimensional distributions of air temperature based on the GMS Standard Atmosphere (monthly climatological data set prepared by the Japan Meteorological Agency, JMA). The daily values of air temperature for evaluating the cloud amounts are determined by linear interpolation of the monthly mean data. Since the discussion will consider the cloud amounts around the Japan Islands, CA7 and CA4 are calculated for the domain of 40°N to 15°N/110°E to 140°E. The present study will use mainly CA7 to identify the cloud area. The daily value of upper-air observation data at the grid points interpolated by the operational Northern Hemisphere Objective Analysis System of the JMA (referred to as ANLMON, hereafter) are used for examining the large-scale circulations (381 km×381 km at 60°N).

3. Formation of the quasi-stationary cloud zone

3.1 Time sequence of the cloud area from April to May

Figure 1 shows the distributions of monthly mean CA7 and equivalent potential temperature, θ_e, at 850 mb in April (in (a)) and May 1979 (in (b)). θ_e is based on ANLMON. The zone with the maximum CA7 extends zonally to the south of the Japan Islands by April. The horizontal gradient of θ_e across the cloud zone is very large in both months. As shown by earlier studies (*e.g.*, Ninomiya and Muraki, 1986), the high value of θ_e (*e.g.*, more than 340 K) is observed just to the south of this cloud zone in May and the cloud zone is identified as the Baiu front (as for the boundary of the cloud zone, see the contour of monthly mean CA7 = 50 %). In April, θ_e just to the south of this cloud zone is slightly smaller, *i.e.*, 335–340 K at ~20°N. In the present study we will refer to this cloud zone, or large $\nabla\theta_e$ zone, identified by the monthly mean fields simply as the frontal zone.

Figure 2 shows the time-latitude section of the area where CA7 averaged from 128°E to 132°E exceeds 5 % (thinly shaded area). That of CA4 ≥ 50 % is also shown as a thickly shaded area in the figure. The stability for moist convection, which is defined by $(\theta_{e500}-\theta_{e900})$ at 00 GMT, at the four upper-air observation stations (Fukuoka, Kagoshima, Naze and Naha) along ~130°E were examined for April and May, where the subscripts 500 and 900 indicate the pressure levels in mbs. The periods when $(\theta_{e500}-\theta_{e900})<0$ (unstable) and those when $(\theta_{e500}-\theta_{e900})\geq 5$ K (highly stable) are also shown in this figure using broken lines and solid lines, respectively (See Section 3.3).

Although the area where CA7 ≥ 50 % increases and extends northward to about 40°N within an interval of a few days in April, the cloud amount decreases rapidly after these peaks. According to daily weather maps (see 3.2), the northward extention of the area with large CA7 corresponds to the passage of a synoptic-scale (or larger meso-α-scale) extratropical cyclone and the area with large CA4 also appears then. On the other hand, the area with large CA7 tends to persist in May, especially after ~15 May the cloud area stagnates without passage of synoptic-scale (or larger meso-α-scale) cyclones to the north of ~30°N. Although the peaks of CA7 also appear in May in association with the disturbances, the area with large CA7 moves southward after the passage of the disturbances and is sustained around 25°N. The cloud area is quasi-stationary in June, as in May. The cloud zone corresponding to the Baiu front shifts northward to ~33°N on ~15 June at ~130°E. It is interesting that the area of CA4 ≥ 50 % is more frequently observed in June.

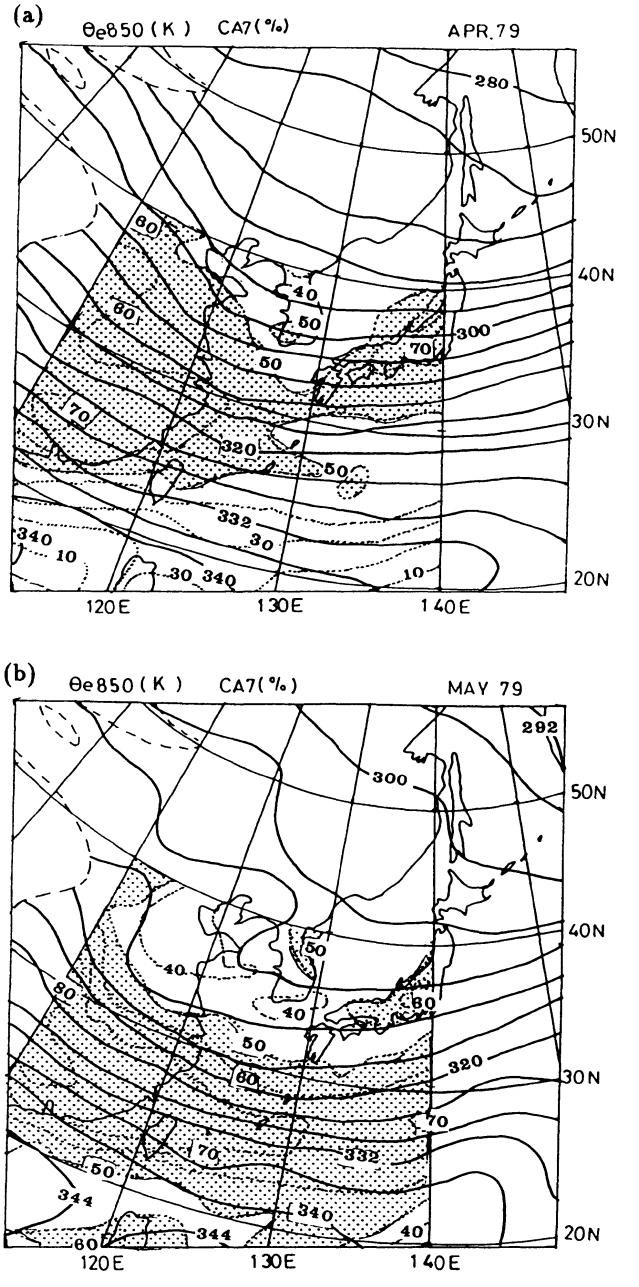

Fig. 1. (a) and (b) Distribution of the monthly mean CA7 (%, dotted lines) and θ_e (K, solid lines) in April and May 1979, respectively. The shaded areas indicated that CA7 exceeds 50 %. The smoothed topography for 1500 m is shown by broken lines. CA7 is calculated within the domain of 15°N–40°N/110°E–140°E. The broken dotted line at 15°N indicates the southern boundary of the domain where CA7 is calculated.

Since the 1°×1° latitude/longitude domain would be overcast by the cloud system associated with the synoptic-scale extratropical cyclones or front, the day-to-day variations of the number of grid points at

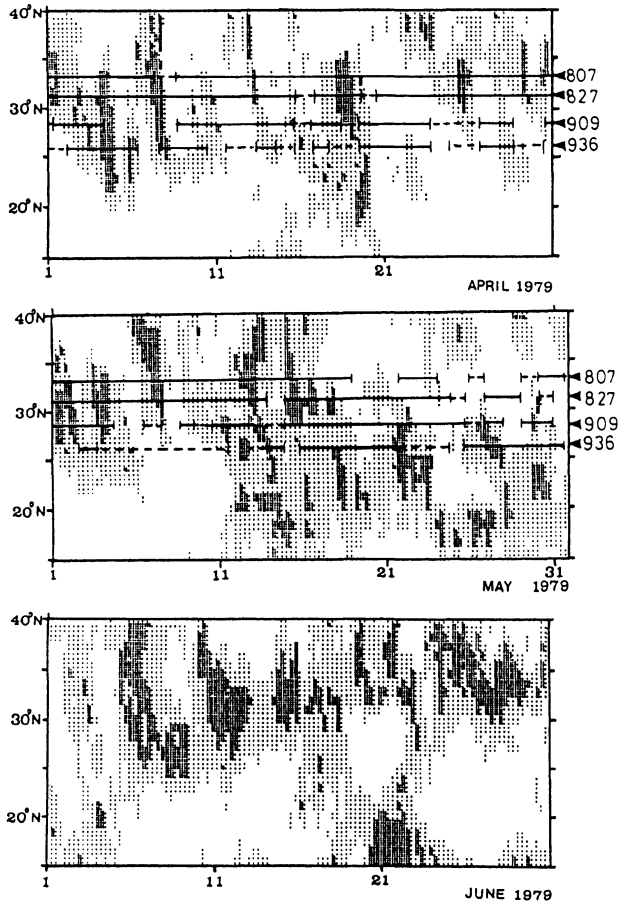

Fig. 2. Time-latitude section of the areas where CA4≥50% and CA7≥50% (CA4 and CA7 are averaged from 128°E to 132°E). The thickly shaded area corresponds to that of CA4 and the thinly one to that of CA7. The upper, the middle and the bottom panels are for April, May and June 1979, respectively. Solid lines indicate the periods when $(\theta_{e500}-\theta_{e900})$ ≥5 K (considerably stable) at each station. Broken lines indicate those when $(\theta_{e500}-\theta_{e900})<0$ (unstable). The data for stability are based on the upper-air observations at 00 GMT at the stations Fukuoka (47807, 33°35′N/130°23′E), Kagoshima (47827, 31°38′N/130°36′E), Naze (47909, 28°23′N/129°33′E) and Naha (47936, 26°12′N/127°41′E).

which CA7≥80% ("cloudy area") will be examined (referred to as GCL). The time sequence of the ratio of GCL to the total number of the grids (RGCL) for the domain 40°N–18°N/125°E–135°E is shown in Fig. 3. The domain is adopted so as to nearly cover the entire region of the daily cloud area corresponding to the frontal zone. The broken line at 25% indicates that the width of the "cloudy area" in the meridional direction is about 600 km if it is uniformly distributed in the zonal direction.

In April the RGCL decreases to nearly 0% after the distinct peaks of the RGCL (passages of extratropical cyclones) with a period of a few days (referred to as "day 0"). This indicates that the "cloudy area" associated with the cloud system on a scale of more than 1°×1° latitude/longitude sometimes tends to disappear in April (this is not the southward shift of the "cloudy area" out of this domain). However, the "cloudy area" to the south of Japan remains even after the peaks in May. Thus we can recognize that the frontal zone at ~130°E became quasi-stationary at the beginning of May 1979 during the seasonal march.

3.2 Behavior of the "cloudy area" during the few days after the passage of a disturbance

Next we will examine the horizontal distributions of the "cloudy area". Figures 4a and 4b present the sequences of GMS Infra-Red pictures including "day 0" as typical examples for April and May, respectively ((a): 12 GMT 19–12 GMT 21 April 1979, (b): 12 GMT 13–00 GMT 15 May 1979). After the passage of the cloud system corresponding to the extratropical cyclone around Kyushu (~33°N/130°E), the clear area expands rapidly there and the cloud belt corresponding to the cold front behind the disturbance disappears as it moves southward in April. This is due to the appearance of an anticyclone moving eastward at the surface level (see Fig. 5a). On the other hand, the cloud belt associated with the synoptic-scale stationary front is sustained even after the passage of the disturbance in May (Fig. 5b).

In order to examine the more general features of the evolution of the cloud distribution after the passage of disturbances, the composite maps of CA7 from "day 0" to "day +2" (two days after "day 0") in April and May, respectively, are presented in Fig. 6. Only the areas where CA7≥60% (referred to as "composite cloudy areas") and CA7≤20% ("cloud free areas") are shown. The map times for the samples corresponding to "day 0" are listed in Table 1 (four cases were picked out for each month). The "day 0" is selected so as to be 00 GMT or 12 GMT when the ANLMON data are available. The distributions of the composite sea level pressure, PSEA, are also presented in these figures.

The "composite cloudy area" is widely distributed corresponding to the pressure depression on "day 0" in April. As the anticyclone moves eastward, the "composite cloudy area" disappears rapidly from "day +1" to "day +2". However, the belt-shaped "composite cloudy area" remains along the southern edge of the anticyclone on "day +1" and "day +2" in May.

Some readers might wonder why the "cloudy area" does not disappear after the passages of dis-

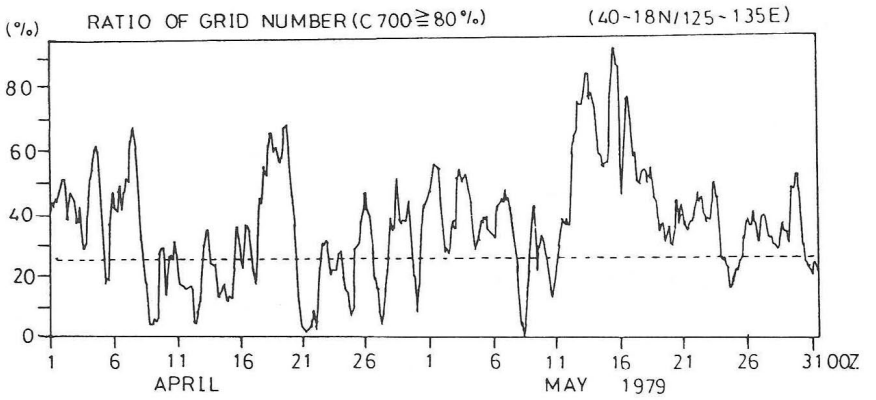

Fig. 3. Time sequence of RGCL for the domain of (40°N to 18°N/125°E to 135°E). The broken line at RGCL of 25 % illustrates that the width of the "cloudy area" in the meridional direction is about 600 km if it is uniformly distributed in the zonal direction.

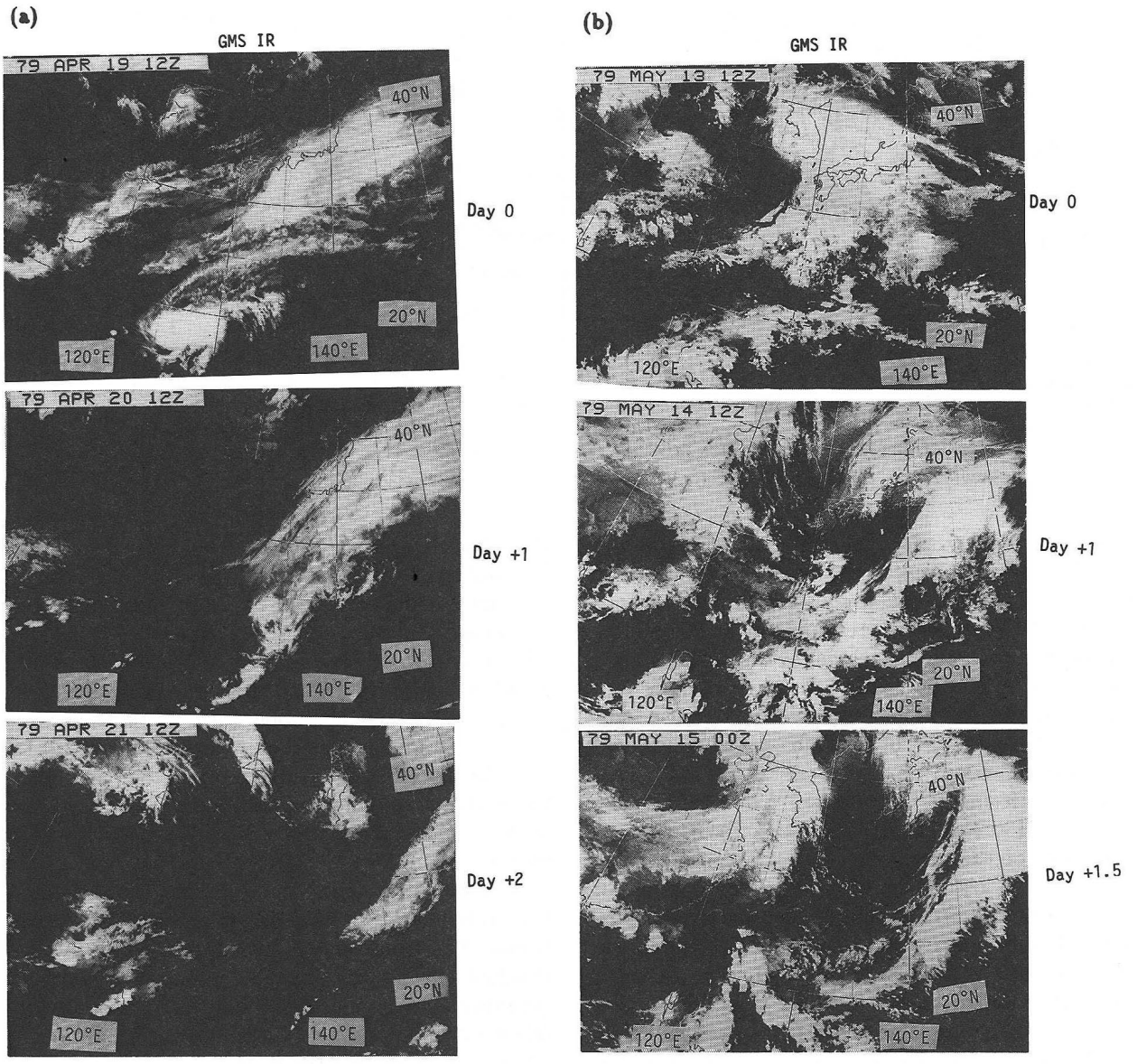

Fig. 4. (a) and (b) Examples of the sequences of GMS Infra-red pictures commencing from "day 0" for April and May 1979, respectively.

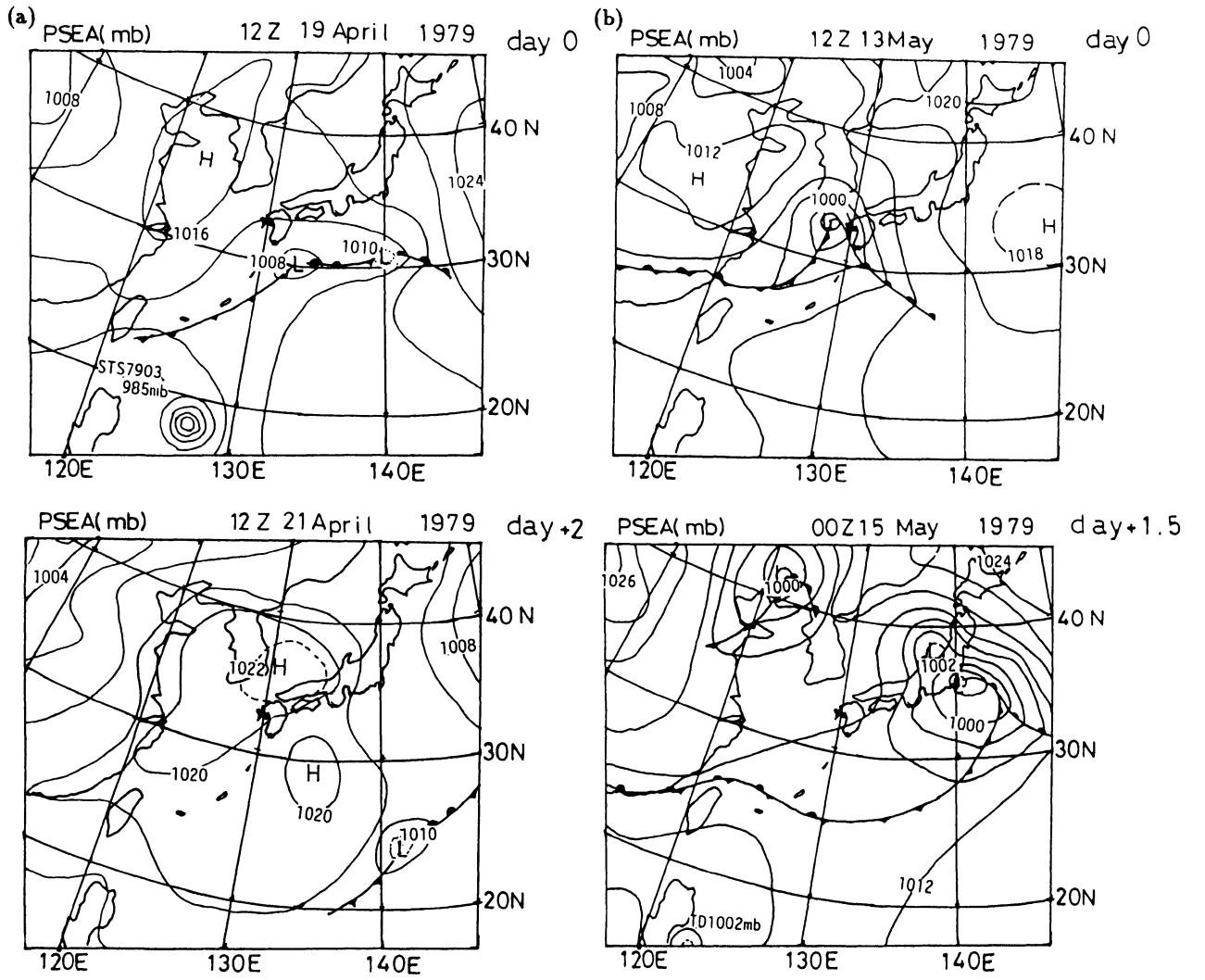

Fig. 5. Distributions of the sea surface pressure on each day presented in Fig. 4. Those on "day +1 are not shown here.

turbances in May, although the anticyclone is also observed behind them. An example of the sequence of surface weather maps shows that the contour of 1016 mb (roughly corresponding to the southern boundary of the anticylone) extended southward to ~20°N/130°E on "day +2" in April (Fig. 5a). The sequence of composite maps (Fig. 6a) also indicates that the contour of 1014 mb (~the boundary of the anticyclone on "day +1" and "day +2") moved southward from ~25°N ("day +1") to ~18°N ("day +2") at ~130°E. On the other hand, the southward extension of the southern edge of the anticyclone is limited to ~27°N in May (*e.g.*, the contour of 1012 mb for Fig. 5b and that of 1014 mb for Fig. 6b). These facts suggest that the anticyclone behind the disturbance has a wider meridional scale in April, while it extends mainly in zonal direction to the north of ~27°N in May. Thus it is concluded that the frontal zone to the south of the Japan Islands in May is not destroyed by the migratory anticyclones.

3.3 Monthly mean fields of low-level temperature and wind

Figure 7 indicates the monthly mean fields of air temperature and wind (vector mean) at 850 mb (T850 and $\boldsymbol{V}850$, respectively). The temperature gradient across the frontal zone in April is stronger than in May and the zone with the strong temperature gradient extends further northward up to ~45°N. The effect of the difference of the baroclinicity on the development of the migratory anticyclone between the two months will be discussed in Section 4.

Now we will examine the frontogenesis of the potential temperature field due to the monthly mean fields. The frontogenesis FG is defined as the individual change of potential temperature gradient (Palmen and Newton, 1969) and is expressed by the following equations (see Nimomiya (1984), although he calculated FG for the θ_e field:

$$FG = \frac{d}{dt}|\nabla\theta| = FG1 + FG2 + FG3 + FG4, \quad (1)$$

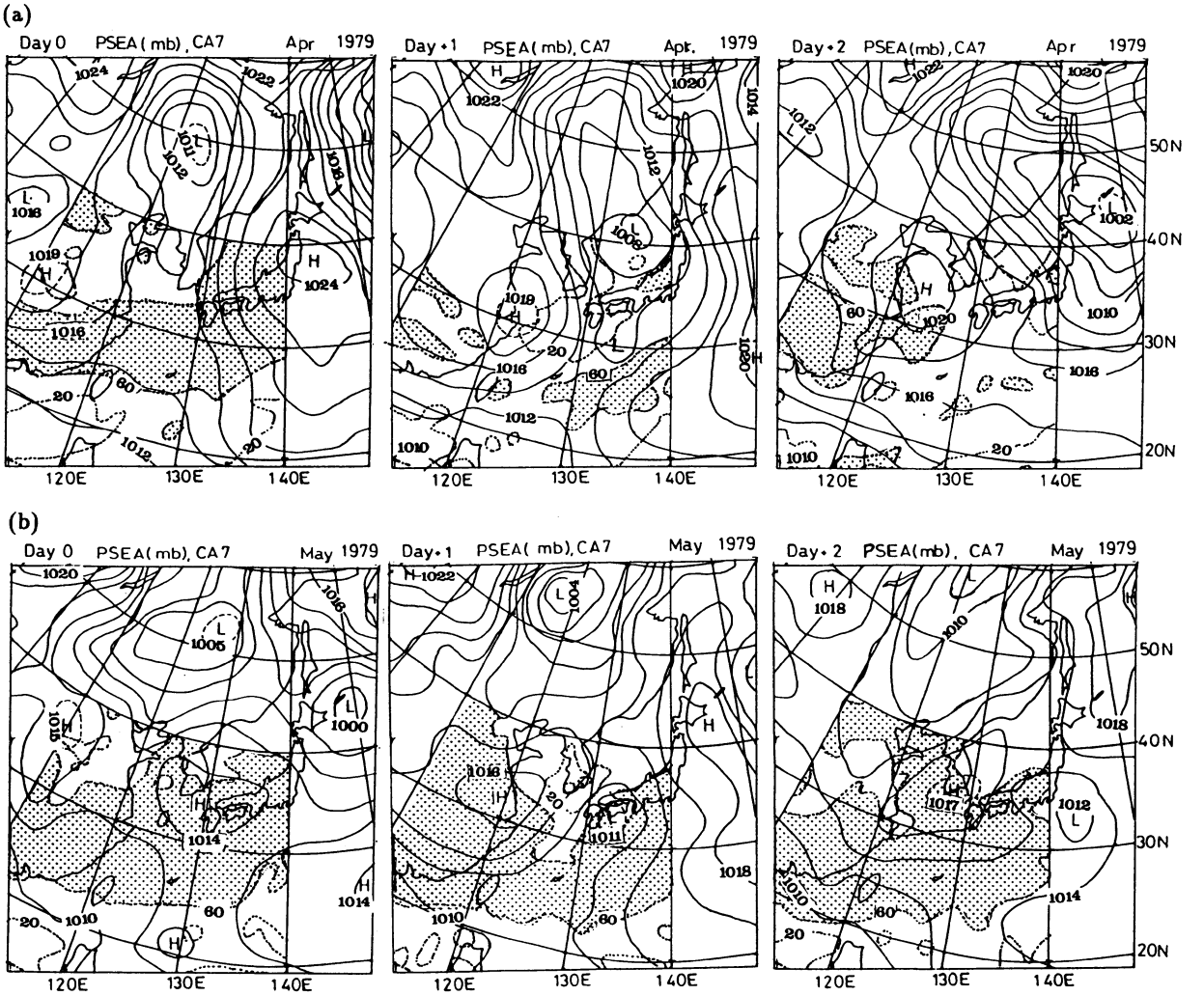

Fig. 6. (a) and (b) Sequences of the composite maps of PSEA (mb, in solid lines) and CA7 (%, in broken lines) in April and May, respectively. The contours of CA7 are shown only for 60 % and 20 %. The shaded areas indicate that CA7 exceeds 60 %.

where

$$FG1 = \frac{1}{|\nabla\theta|}\left[(\nabla\theta)\cdot\nabla\left(\frac{d\theta}{dt}\right)\right], \tag{2}$$

$$FG2 = -\frac{1}{2}\frac{1}{|\nabla\theta|}(\nabla\theta)^2 D, \tag{3}$$

$$FG3 = -\frac{1}{2}\frac{1}{|\nabla\theta|}\left[\left\{\left(\frac{\partial\theta}{\partial x}\right)^2-\left(\frac{\partial\theta}{\partial y}\right)^2\right\}A + 2\frac{\partial\theta}{\partial x}\frac{\partial\theta}{\partial y}B\right], \tag{4}$$

and

$$FG4 = -\frac{1}{|\nabla\theta|}\frac{\partial\theta}{\partial p}\left(\frac{\partial\theta}{\partial x}\frac{\partial\omega}{\partial x}+\frac{\partial\theta}{\partial y}\frac{\partial\omega}{\partial y}\right). \tag{5}$$

θ is potential temperature and the other notations are conventional. D is the horizontal divergence. $A = \partial u/\partial x - \partial v/\partial y$ and $B = \partial v/\partial x + \partial u/\partial y$ are deformations. $FG1$ is due to the diabatic heating. $FG2$ and $FG3$ are due to the horizontal divergence and the deformations, respectively, and $FG4$ to the vertical motion. Since it is very difficult to evaluate the diabatic heating rate and the vertical motion by using the observational data, we will examine only $FG2$ and $FG3$ by using the time mean fields of θ and $\boldsymbol{V}$ at 850 mb level.

Table 1. List of map times on "day 0" used for the composite analyses for April and May 1979.

April	May
12 GMT 7 April	12 GMT 1 May
12 GMT 13 April	12 GMT 3 May
00 GMT 16 April	12 GMT 9 May
12 GMT 19 April	12 GMT 13 May

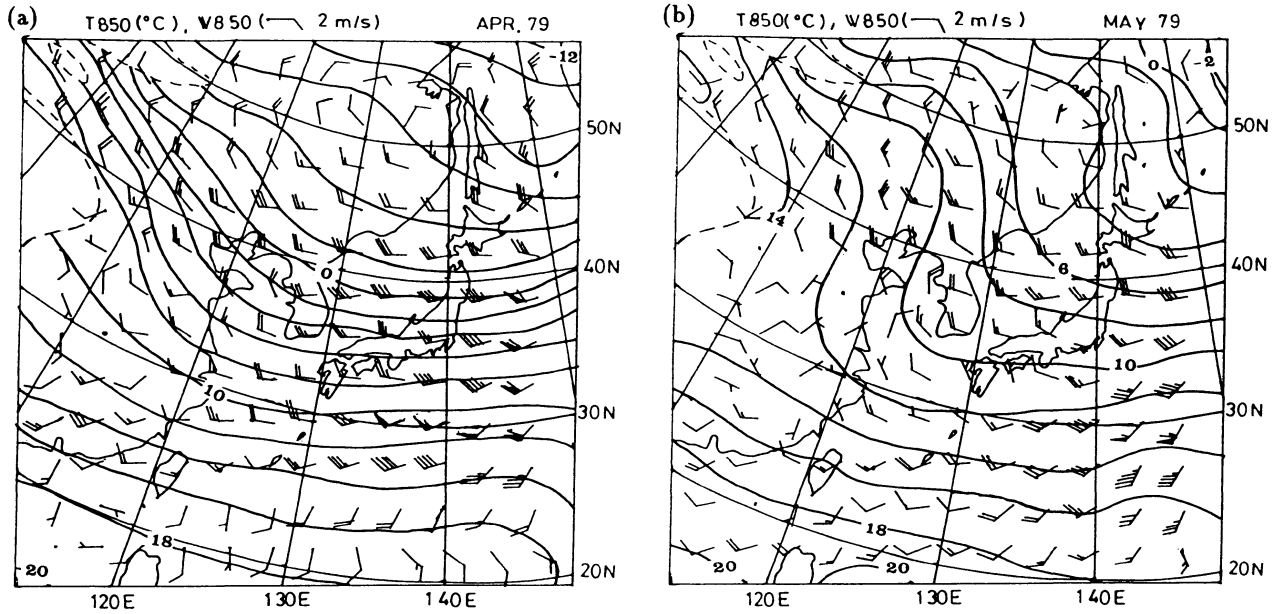

Fig. 7. (a) and (b) Distribution of the monthly mean T850 (°C, in solid lines) and V850 in April and May 1979, respectively. A full barb indicates 2 ms^{-1} and a half barb 1 ms^{-1}. a flag denotes 10 m s^{-1}.

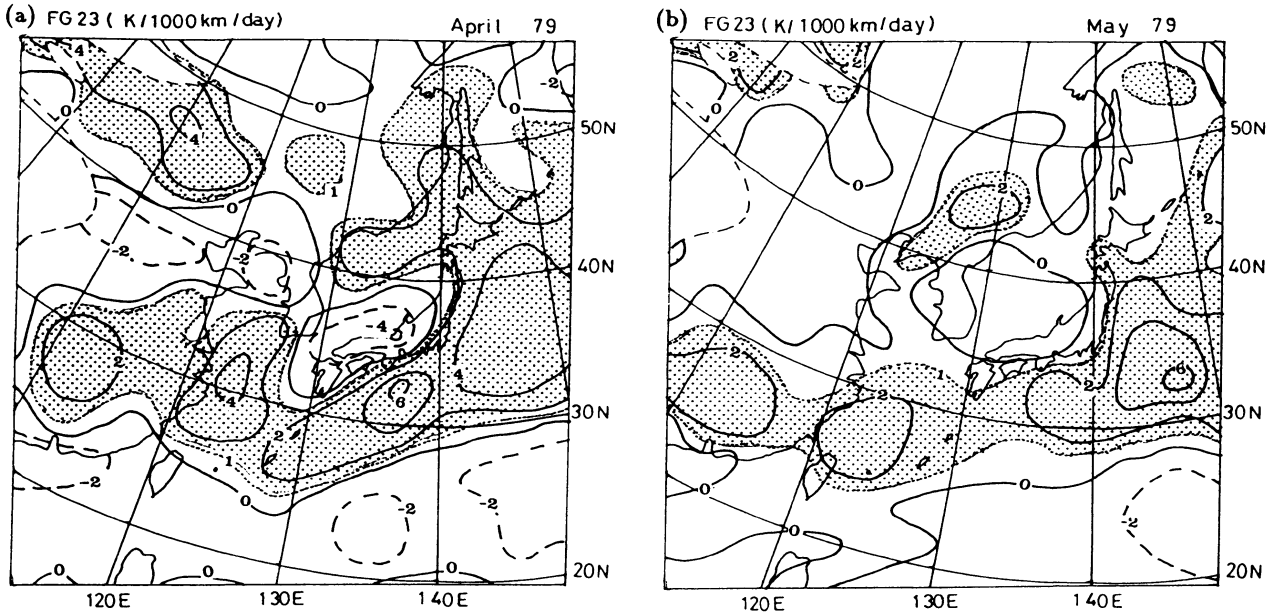

Fig. 8. Distribution of ($FG2$+$FG2$) at 850 mb level calculated by the monthly mean fields (K (1000 km)$^{-1}$ day^{-1}). Shaded areas indicate that ($FG2$+$FG3$) $\geq$ +1 K (1000 km)$^{-1}$ day^{-1}. The contours for negative values are shown by broken lines.

Figures 8a and 8b show the distributions of ($FG2$ +$FG3$) in April and May, respectively. Although the figure is not shown here, $FG3$ is the dominant term in most areas in Fig. 8. We find the zone of frontogenesis due to the horizontal motion to be roughly along the frontal zone, corresponding to the confluence of the southwesterly wind and the northwesterly (or westerly) wind in the lower layer in both months. Although the temperature gradient across the front, and ($FG2$+$FG3$) are small in May compared to those in April, it is noted that the monthly mean temperature and the wind fields at 850 mb level cause frontogenesis also in May.

Figure 9 shows the distributions of T850 and V850 on 12 GMT 14 May as an example for "day +1" in May. The confluence of the SSW-ly and the NW-1y (or ENE-1y) winds along the stationary front (~27°N) on the 850 mb map by JMA is found across the belt-shaped cloud zone to the west of ~130°E (Fig. 4b). It is interesting that the circu-

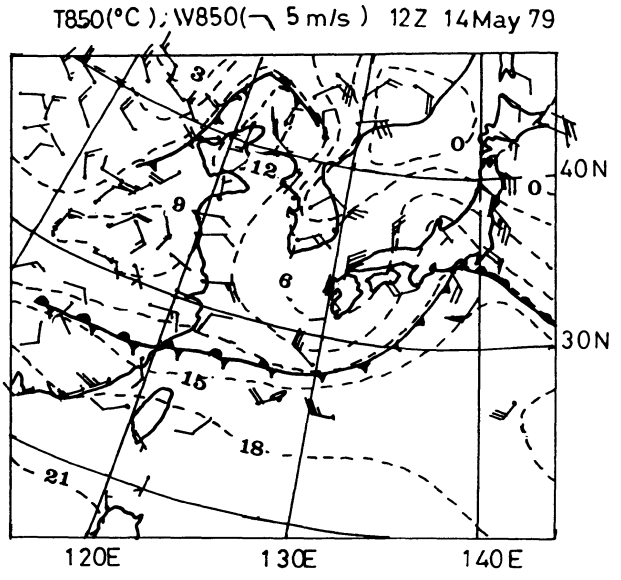

Fig. 9. Distribution of T850 (°C) and $V850$ on 12 GMT 14 May as an example for "day +1" in May (the GMS pictures at the same time are referred to in Fig. 7b. A full barb indicates 5 m s^{-1} and a half barb 2.5 m s^{-1}.

lation pattern around the stationary front resembles the monthly mean one (Fig. 7b).

As mentioned in 3.2, the migratory anticyclones do not destroy the stationary front and the frontogenesis in the lower layer due to the monthly mean horizontal fields seems to contribute to the maintenance of quasi-stationary frontal zone in May (the cloud zone which appears on "day +1", "day +2", and the period after ~15 May).

It is also noted that the stratification in the daily cloud zone is highly stable against moist convection in both April and May (frequent appearance of the case $(\theta_{e500}-\theta_{e900}) \geq 5$ K), except for some cases associated with "day 0", and so on[1] (Fig. 2). Although deep convective clouds are also observed in the southern part of the frontal zone in May (Ninomiya, 1989), the frontal zone in May is characterized as a baroclinic zone with the stable stratification against moist convection. In the present study the daily values of frontogenesis were not estimated due to the accuracy of the data. However, it will be necessary to examine them for "day +1", "day +2" and the period after ~15 May in future studies.

4. Seasonal transition of the temperature field in East Asia from April to May

Figure 10 shows the distributions of monthly mean geopotential height at 500 mb (Z500) and

[1]Frequent appearance of the unstable cases at Naha (the southernmost station) is partly due to the northward shift of the frontal zone and it was covered with the subtropical high (*e.g.*, 7 to 10 May).

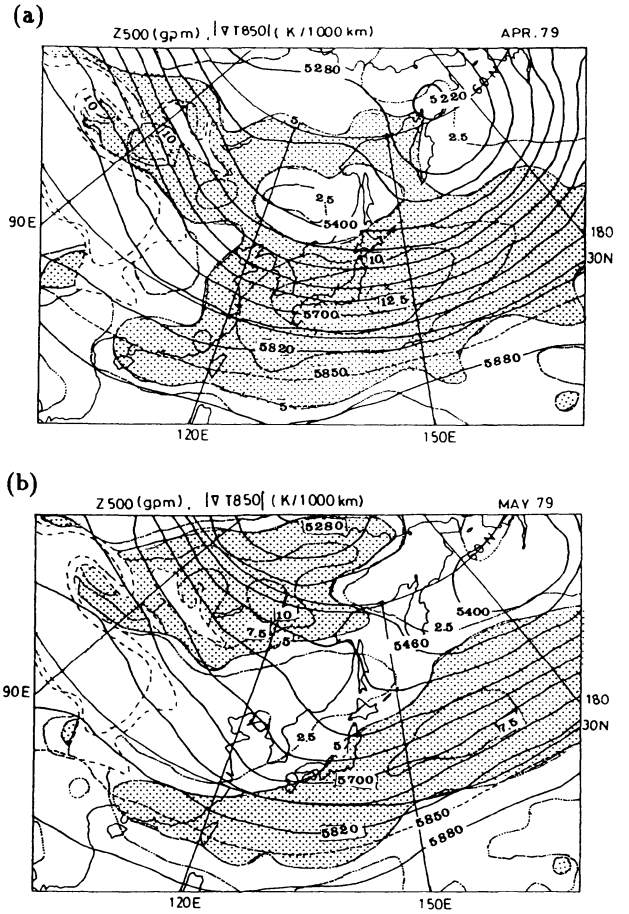

Fig. 10. Distribution of the monthly mean Z500 (gpm, in solid lines) and $|\nabla\overline{T850}|$ (K (1000 km)$^{-1}$, in dotted lines). (a): April 1979 and (b): May 1979. The areas where $|\nabla\overline{T850}| \geq 5$ K (1000 km)$^{-1}$ are shaded.

the magnitude of the horizontal gradient of monthly mean T850 ($|\nabla\overline{T850}|$) in April and May 1979. The areas where $|\nabla\overline{T850}| \geq 5$ K (1000 km)$^{-1}$ are shaded.

In April the northern and the southern branches of the westerly jet at 500 mb around the Tibetan Plateau are confluent with each other at ~115°E, and the westerly jet is stronger in the vicinity of the Japan Islands (~140°E), as suggested by the Z500 field. The baroclinicity in the lower layer is very strong around the frontal zone to the south of the Japan Islands (the peak of $|\nabla\overline{T850}|$ attains 13 K (1000 km)$^{-1}$) and the area with such a strong temperature gradient has a considerable width in the meridional direction (*e.g.*, the area where $|\nabla\overline{T850}| \geq 5$ K (1000 km)$^{-1}$ extends from 20°N to 45°N).

On the other hand, the baroclinic zone corresponding to the Baiu front is weakened and becomes narrower in May (20°N–35°N). Another area with a high temperature gradient in the lower layer is found to the north of the Tibetan Plateau (~55°N/110°E) (the polar frontal zone in the eastern part of Siberia corresponding to the northern branch of the middle-

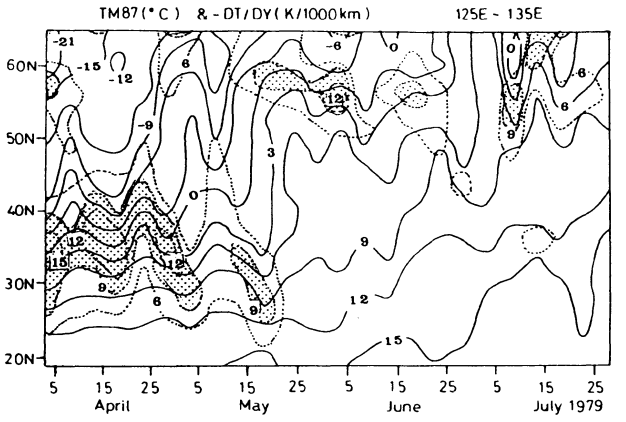

Fig. 11. Time-latitude section of 5-day mean TM87 (°C, in solid lines) and GR87 (K (1000 km)$^{-1}$, in dotted lines) averaged from 125°E to 135°E in 1979. The shaded areas indicate that GR87 is greater than 9 K (1000 km)$^{-1}$.

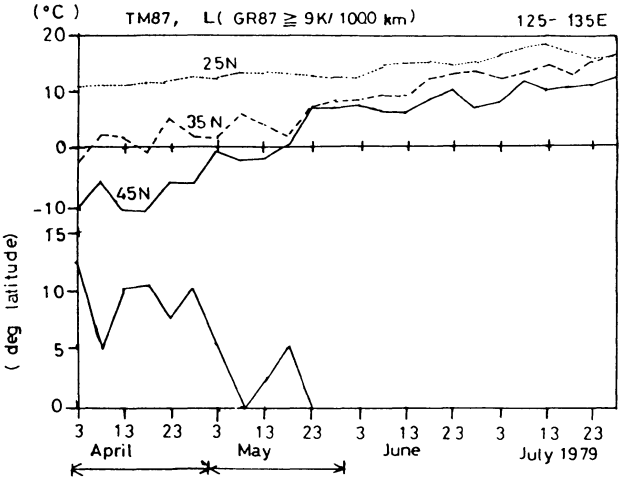

Fig. 12. 5-day mean TM87 at 25°N (a dotted line), 35°N (a broken line) and 45°N (a solid line) averaged from 125°E to 135°E, and the meridional width of the area where GR87 is greater than 9 K (1000 km)$^{-1}$ derived from Fig. 11 (the lower part of this figure), in ° latitude.

level westerly jet). However, the two baroclinic zones are separate from each other, which results in the weakening of baroclinicity just to the north of the Baiu front in May.

Comparing the T850 fields between April and May (Fig. 7), T850 in higher latitudes is larger over the Asian continent than over the northwestern Pacific. For example, the contour T850=8°C shifted from ~34°N (in April) to ~50°N (in May) at 115°E, while from ~33°N (in April) to ~37°N (in May) at ~140°E. The change in the baroclinicity over East Asia from April to May is associated with the difference of the temperature rise between the continent and the ocean. However, the quantitative analyses such as of the heat budget and the all of the terms of frontogenesis ($FG1 \sim FG4$) are needed in future in order to understand the effects of this thermal contrast.

Figure 11 presents the time-latitude section of the 5-day mean air temperature in the layer from 700 mb to 850 mb level (TM87) averaged from 125°E to 135°E in early summer of 1979 (in solid lines). The meridional gradient of TM87, $-\frac{1}{a}\frac{\partial}{\partial\phi}$TM87 (GR87), is also shown by dotted lines, where a and φ denote the radius of the earth and the latitude, respectively. The time sequences of the 5-day mean TM87 at 25°N, 35°N and 45°N averaged from 125°E to 135°E, and the meridional width of the area where GR87 $\geq$ 9 K (1000 km) derived from Fig. 11, are shown in Fig. 12.

Kato (1985a, 1987) showed that the temperature gradient around the Baiu front over the continent vanished abruptly in late May of 1979. At that time the air temperature to the north of the Baiu front near the Japan Islands (~40°N) increased rapidly and GR87 across the front decreased considerably (Fig. 11). GR87 weakened and the meridional width of the baroclinic zone (*e.g.*, GR87 $\geq$ 9 K/1000 km) decreased also at the beginning of May, mainly due to the temperature rise to the north of ~40°N (Fig. 12). Thus we should note that the weakening of baroclinicity across the front and in the adjacent area to its north, and the separation from the polar front, occurred about a month before the abrupt disappearance of the temperature gradient across the Baiu front in China pointed out by Kato (1985a, 1987).

5. Effects of the change in baroclinicity between April and May

Figures 13a and 13b present the 500 mb maps around Japan at 12 GMT 19 April and 12 GMT 13 May 1979, respectively, as the examples on "day 0" (the same dates as in Figs. 4 and 5). As for Fig. 12a, the 500 mb maps on "day −1" and "day +1" are shown together. The location of the surface-level front in question is indicated on these maps. The readers are also referred to Fig. 4 and 5.

The synoptic-scale extratropical cyclone at the surface level, which appeared at ~27°N/122°E on "day −1" (18 April) (not shown here), developed as it moved eastward. The center pressure of the migratory anticyclone behind the cyclone increased by 6 mb from "day 0" to "day +2" (1016 mb on "day 0" and 1022 mb on "day +2") and the area surrounded by the contour of 1016 mb expanded rapidly (refer to 3.3 and Fig. 5a). The 500 mb trough with a wide meridional extension (25°N–50°N) is located westward from the center of the cyclone at the surface

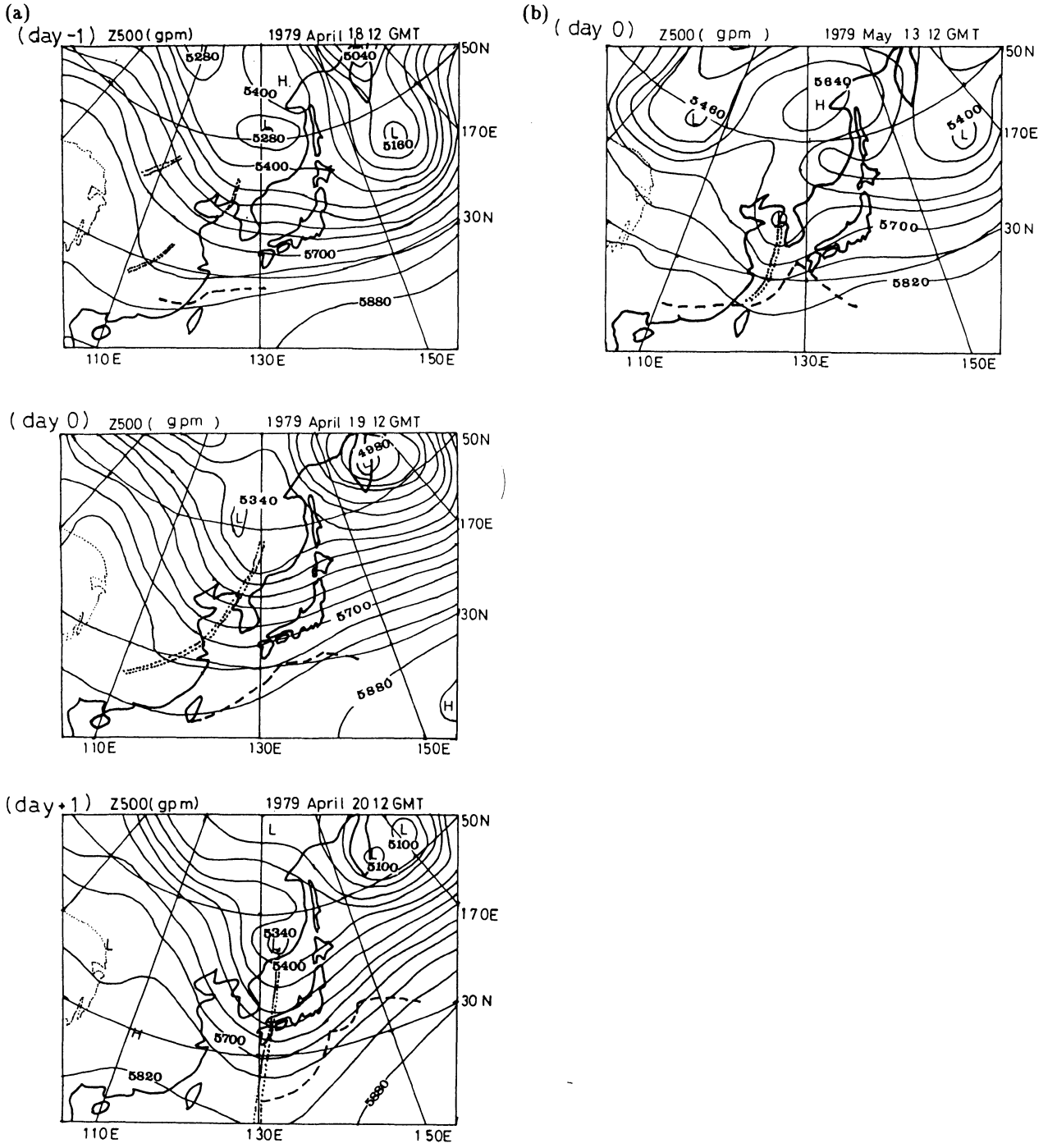

Fig. 13. Distributions of Z500 (gpm) at 12 GMT 19 April and 12 GMT 13 May 1979 are presented in (a) and (b), respectively, as the examples for "day 0" (the same dates as in Figs. 4 and 5). The locations of the surface-level front and the 500 mb-level trough near the southern part of Japan are shown by a thick broken line and two thick dotted lines. As for (a), the similar maps on "day −1" and "day +1" are attached.

level by about 1000 km on "day 0" in April. Thus the development of the migratory anticyclone is suggested to be due to the baroclinic instability. It is noted that the rapid development of the trough at the 500 mb level in April occurred after it reached around the western part of the Japan Islands, where the area with a strong temperature gradient (*e.g.*, $|\nabla\overline{T850}| \geq 7.5\,\mathrm{K}\ (1000\,\mathrm{km})^{-1}$) expanded widely in the meridional direction (to the east of ~120°E) as mentioned in Section 4.

Figure 14 illustrates the composite maps of Z500 from "day 0" to "day +2" for the same samples as

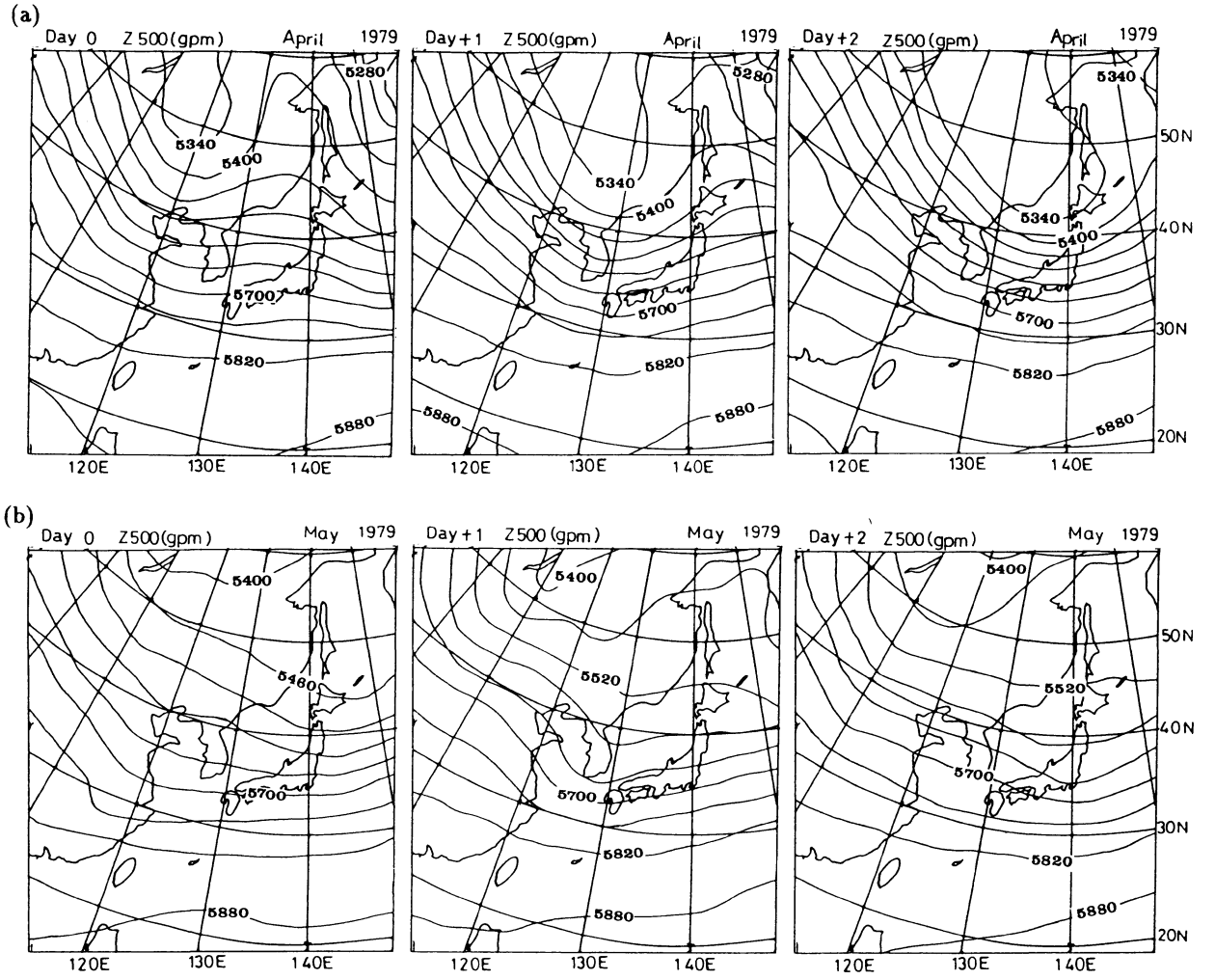

Fig. 14. Sequences of the composite Z500 maps from "day 0" to "day +2" (gmp) based on the samples listed in Table 1. (a): April, and (b): May.

in Fig. 6. The migratory anticylone develops around the western part of Japan in April, corresponding to the rapid enhancement of the 500 mb trough with a wide meridional extension, as revealed by the typical case shown in Figs. 5a and 13a. On the other hand, the 500 mb trough corresponding to the low at the surface level on "day 0" in May is not so deep and the northward extension of the 500 mb trough is limited to ~40°N within the relatively narrow baroclinic zone in May (see Figs. 13b and 14b).

Figure 15 presents the composite maps of the locations of the fronts and the centers of anticyclones in the twice-daily surface weather maps issued by the JMA for the three periods of 11 to 20 April, 1 to 10 May and 21 to 31 May 1979. The centers of anticyclones appear nearly in the same region as the surface-level fronts in April (25–40°N), which is consistent with the development of anticyclones there due to the baroclinic instability.

In May, however, the surface-level front (the Baiu front) tends to appear at ~25°N, just to the south of the region where the centers of anticyclones are observed (30–40°N). Furthermore, the zone with high appearance frequency of the front at ~25°N (the Baiu front) and that at ~50°N (the polar front) do not meet with each other around the Japan Islands. In other words, the disturbance on the polar frontal zone can not be coupled with that on the polar frontal zone into a synoptic-scale baroclinic wave around Japan in May. Thus we can conclude that the weakening of the baroclinic zone and its separation into the two branches around Japan contribute to the formation of the quasi-stationary Baiu front at the beginning of May, by suppressing the development of a migratory anticyclone as the baroclinic wave.

Now one may have a question: why the cyclones sometimes appear on the frontal zone around the Japan Islands in May in spite of the decrease in the baroclinicity there? Murakami and Huang (1984) examined the effects of the Tibetan Plateau on the rainfall variations in Central China during early summer of 1979. They showed that the disturbance which brings the distinct peak of precipita-

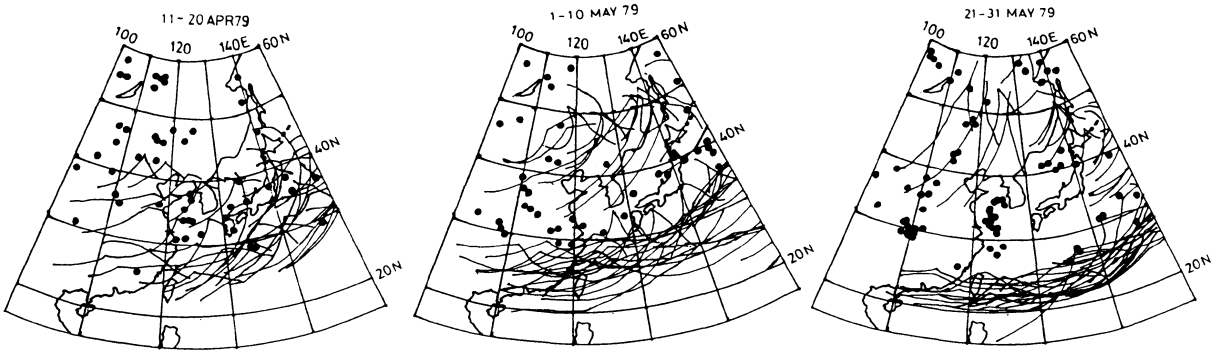

Fig. 15. Composite distributions of the locations of the front and center of the anticyclone on the twice-daily surface weather maps issued by the JMA for the periods of 11–20 April, 1–10 May and 21–31 May 1979. The surface front and the center of the anticyclone are illustrated by a thick solid line and a black circle, respectively.

tion in Central China before the onset of the Indian Monsoon (May to early June) is generated at the northeastern edge of the Tibetan Plateau by mechanical effects (not thermal ones). Then this low-level edge cyclone merges with an eastward-propagating upper-level trough and moves further eastward. They suggested that the cyclone resembles a wintertime edge cyclone (Murakami, 1981; Murakami and Nakamura, 1983). Although their statistics were made including the two stages before and after the change in the thermal structure of the Baiu front in China (Kato, 1985a, 1987), the Tibetan Plateau would play a role in generating the cyclone which propagates eastward on the Baiu frontal zone in May. The cyclone could not develop into a larger-scale one due to the lack of sufficient baroclinicity around the Japan Islands. The present study can not answer the question mentioned above further. Thus a comparison of the evolution processes of disturbances on the Baiu front between different stages is needed in future.

6. Appearance of the quasi-stationary front in the other years

Figure 16 shows the day-to-day variation of the location of front on twice-daily surface maps (00 GMT and 12 GMT), issued by the JMA, at 130°E in April and May of 1979, 1985, 1986, 1987, and 1988. The periods when the surface front is continuously analyzed for more than 5 map times between 16°N and 37°N at 130°E are also shown by bars at the bottom (the number of map times in this continuous appearance of the front is referred to as NSS).

The surface front often at first appears around 30–40°N in April, which would be due to the passage of the synoptic-scale (or larger meso-α-scale) disturbance. Then it moves southward and disappears. However, after the date indicated by a dotted line in each year, once the front appears in this region, it tends to stagnate around ~25°N for more than a few days (quasi-stationary character). These features are typical in 1979. As for the figure in 1979, the quasi-stationary behavior of the front mentioned above is consistent with that of the large CA7 area in Fig. 2.

Next we will calculate the following quantities for April and May, respectively:

$$RSS = (NSS/NTM) \times 100(\%), \tag{6}$$

$$RFF = (NFF/NTM) \times 100(\%) \tag{7}$$

and

$$RSF = (NSS/NFF) \times 100(\%), \tag{8}$$

where NFF is the number of all the map times when the front appears between 16°N and 43°N at 130°E, regardless of its properties. NTM is the total number of map times for the analysis period. When more than two fronts were analyzed at the same time, we counted it as one event. Based on the weather maps from 00 GMT 1 April to 12 GMT 31 May in each year, the statistics are for events from 00 GMT 3 April to 12 GMT 27 May. The results are presented in Table 2.

In May, RSS and RFF are greater than in April. It is noted that about 80% of the front in May shows the quasi-stationary character (see the value of RSF). The climatological studies by Yamakawa (1988), Yoshino and Yamakawa (1985), which are based on the daily weather maps for about 40 years, showed that the appearance frequency of a "stationary front-type pressure pattern" increases gradually from April to June, but the "pressure pattern of zonal high belt" extending from Central China to the east of the Japan Islands appears also frequently in May.

Takeda and Ikeyama (1985) reported that a large amplitude of the 30-day variation of cloud amount is found in the middle latitude just to the south of Japan, as well as in tropics. They suggested

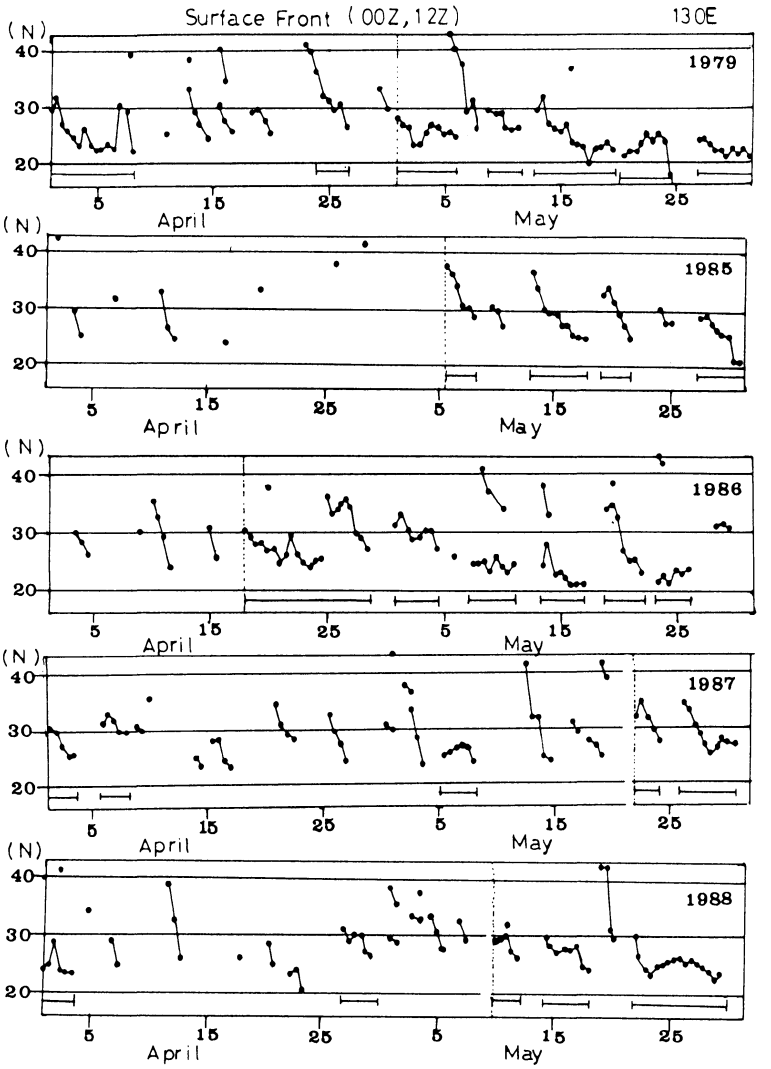

Fig. 16. Day-to-day variation of the location of the front on twice-daily surface maps at 130°E from April to May of 1979, 1985, 1986, 1987 and 1988. The periods when the surface front is continuously analyzed for more than 5 map times between 16°N and 37°N at 130°E are also shown by bars.

that the maximum anomaly of the 30-day variation just to the south of Japan in the warmer season is partly due to the frequent appearance of the events when it is almost overcast (associated with the synoptic-scale disturbances or fronts) during its positive anomaly period. Thus the relatively high frequency of the appearance of the "pressure pattern of zonal high belt" mentioned above in May seems to be affected by the 30-day variation. Considering these discussions, it is concluded that the front, once it appears to the south of the Japan Islands, tends to become quasi-stationary after the beginning of May.

7. Summary and conclusions

The formation of the "quasi-stationary" Baiu front to the south of the Japan Islands at the beginning of May and its relation to the seasonal transition of the large-scale baroclinicity in East Asia was examined by using observational data for 1979.

Table 2. Comparison of RSS, RFF and RSF between April and May 1979. Details are referred to in the text.

	RSS (%)	RFF (%)	RSF (%)
April	18	43	42
May	53	68	79

The frontal zone to the south of the Japan Islands, corresponding to the southern branch of the middle-level westerly jet around the Tibetan Plateau, is characterized by the passages of the cloud systems associated with synoptic-scale extratropical cyclones in April. After their passage, the cloud area diminishes in association with the development of the migratory anticyclone. On the other hand, the cloud area associated with the stationary front is sustained

at ~25°N in May even after the passage of the synoptic-scale (or larger meso-α-scale) disturbance at ~30°N. In other words, the frontal zone to the south of the Japan Islands became quasi-stationary at the beginning of May. Since the equivalent potential temperature just to the south of this (time mean) frontal zone reaches about 340 K, the transition at the beginning of May 1979 is regarded as the formation of the "quasi-stationary Baiu front" around Japan (the beginning of Stage A). The analysis of the location of the front on twice-daily surface weather maps in 1985, 1986, 1987 and 1988, as well as 1979, shows that the change into the quasi-stationary frontal zone occurred around early May of the other years.

The two baroclinic zones, corresponding to the southern and the northern branches of the westerly jet, respectively, are separate from each other around the Japan Islands in May because of the seasonal transition, which results in the weakening of baroclinicity just to the north of the Baiu front as well as that across the Baiu front in May. Such a change in the large-scale baroclinicity from April to May tends to suppress the development of the migratory anticyclone as the baroclinic instability wave and a favorable condition exists for sustaining the "quasi-stationary" Baiu front in May, without the cloud zone being destroyed by the anticyclone.

It is noted that the change into the quasi-stationary frontal zone at the beginning of May 1979 revealed in the present study occured a month before the abrupt disappearance of the temperature gradient across the Baiu front in China pointed out by Kato (1985a. 1987). Although these two transitions are related to the larger temperature rise in higher latitudes over the Asian Continent than over the sea in the same latitudes, we should recognize that they are different events in the seasonal march.

The seasonal transition of the large-scale atmospheric circulations around the Baiu front in early summer shows several abrupt steps and the processes which make the Baiu front of quasi-stationary character would be very different between each other stage (Kato, 1985a, 1987, 1989; Ninomiya and Muraki, 1986; Ninomiya, 1989; Akiyama, 1989, 1990a, b). Thus the maintenance processes associated with the quasi-stationary character of the frontal zone in each stage of the seasonal transition should be examined in the future.

Acknowledgements

The authors express their sincere thanks to Prof. Takao Takeda, Water Research Institute of Nagoya University, and Prof. Tomio Asai, Ocean Research Institute of the University of Tokyo for providing valuable comments. They are very grateful to Dr. Masato Murakami, Meteorological Research Institute (MRI), JMA, for permitting use of the histogram data of infrared observations by the GMS compiled by him. In the present study the GANAL data on the magnetic tapes were provided by the Numerical Prediction Division of JMA. They are also grateful to Dr. Takako Akiyama, MRI of JMA, and the two reviewers for providing valuable comments.

References

Akiyama, T., 1973: The large-scale aspects of the characteristic features of the Baiu front. *Pap. Meteor. Geophys.*, **24**, 157–188.

Akiyama, T., 1989: Large, synoptic and mesoscale variations of the Baiu front, during July 1982. Part I Cloud features. *J. Meteor. Soc. Japan*, **67**, 57–81.

Akiyama, T., 1990a: Same as above. Part II: Frontal structure and disturbances. *J. Meteor. Soc. Japan*, **68**, 557–574.

Akiyama, T., 1990b: Same as above. Part III: Space-time scale and structure of frontal disturbances. *J. Meteor. Soc. Japan*, **68**, 705–727.

Dao, S.Y. and L.S. Chen, 1957: The structure of general circulation over continent of Asia in summer. *J. Meteor. Soc. Japan.* 75th Ann. Vol., 215–229.

Gao, Y.X. and S.Y. Xu, 1962: The advance and retreat of the monsoon in East Asia and the beginning and the terminal of the rainy season (in Chinese). *Some problems on the monsoon in East Asia*, 78–87. Japanese edition in "Rain and Climate" (edited by Yoshino, M.M. and K.Y. Chen), Taimeido, Tokyo, 160–170.

Kato, K., 1985a: On the abrupt change in the structure of the Baiu front over the China Continent in late May of 1979. *J. Meteor. Soc. Japan*, **63**, 20–36.

Kato, K., 1985b: Characteristics of the Baiu frontal zone over the China Continent (in Japanese). *Tenki*, **32**, 333–335 (with frontispiece photographs in No. 6 of Tenki, 32).

Kato, K., 1987: Airmass transformation over the semi-arid region around North China and abrupt change in the structure of the Baiu front in early summer. *J. Meteor. Soc. Japan*, **65**, 737–750.

Kato, K., 1989: Seasonal transition of the lower-level circulation systems around the Baiu front in China in 1979 and its relation to the Northern Summer Monsoon. *J. Meteor. Soc. Japan*, **67**, 249–265.

Kodama, Y. and T. Asai, 1988: Large-scale cloud distributions and their seasonal variations as derived from GMS-IR observations. *J. Meteor. Soc. Japan*, **66**, 87–101.

Matsumoto, J., 1984: Summertime circulation patterns over Eastern Asia (in Japanese with English abstract). *Geograph. Rev. Japan* (Ser. A), **57**, 137–155.

Murakami, M., 1983: Analysis of the deep convective activity over the western Pacific and southwest Asia. Part I: Diurnal variation. *J. Meteor. Soc. Japan*, **61**, 60–76.

Murakami, T., 1981: Orographic influence of the Tibetan Plateau on the Asiatic winter monsoon circulation. Part III: Short-period oscillations. *J. Meteor. Soc. Japan*, **59**, 173–200.

Murakami, T. and H. Nakamura, 1983: Orographic effects on cold surges and lee-cyclogenesis as revealed by a numerical experiment. Part II: Transient aspects. *J. Meteor. Soc. Japan*, **61**, 547–567.
Murakami, T. and W.G. Huang, 1984: Orographic effects of the Tibetan Plateau on the rainfall variations over the Central China during the 1979 summer. *J. Meteor. Soc. Japan*, **62**, 895–909.
Ninomiya, K., 1984: Characteristics of the Baiu front as a predominant subtropical front in summer northern hemisphere. *J. Meteor. Soc. Japan*, **62**, 880–894.
Ninomiya, K., 1989: Cloud distribution over East Asia during Baiu period of 1979. *J. Meteor. Soc. Japan*, **67**, 639–658.
Ninomiya, K. and H. Muraki, 1986: Large-scale circulations over East Asia during the Baiu period of 1979. *J. Meteor. Soc. Japan*, **64**, 409–429.
Nitta, Ts., 1986: Long-term variations of cloud amount in the western Pacific region. *J. Meteor. Soc. Japan*, **64**, 373–390.
Palmen, E. and C.W. Newton, 1969: *Atmospheric circulation systems.* Academic Press, 602 pp.
Saito, N., 1966: A preliminary study of the summer monsoon of the Southern and Eastern Asia. *J. Meteor. Soc. Japan*, **44**, 44–59.
Saito, N., 1985: Quasi-stationary waves in mid-latitudes and the Baiu in Japan. *J. Meteor. Soc. Japan*, **63**, 983–995.
Takeda, T. and M. Ikeyama, 1985: Time variation of cloud amount with about 30-day period in the western Pacific region. *J. Meteor. Soc. Japan*, **63**, 997–1012.
Tao, S.Y. and Y.H. Ding, 1981: Observational evidence of the influence of the Qinhai-Xizang (Tibet) Plateau on the occurrence of heavy rain and severe storms in China. *Bull. Amer. Meteor. Soc.*, **62**, 23–30.
Tao, S.Y., S.X. He and Z.F. Yang, 1983: An observational study on the onset of the summer monsoon over Eastern Asia in 1979 (in Chinese with English abstract). *Scientia Atmos. Sinica*, **7**, 347–355.
Yamakawa, S., 1984: Regional and seasonal features of cold fronts in Japan and its surroundings. *Geograph. Rev. Japan*, **57**, (Ser. B), 154–165.
Yamakawa, S., 1988: Climatic variations in recent years from the view point of the seasonal transition of prevailing pressure pattern types over East Asia (in Japanese with English abstract). *Geograph. Rev. Japan*, **61** (Ser. A), 381–403.
Yeh, T.C., S.Y. Dao and M.T. Li, 1959: The abrupt change of circulation over the Northern Hemisphere during June and October. *Atmosphere and Sea in Motion*, 249–267.
Yin, M.T., 1949: A synoptic-aerological study of the onset of the summer monsoon over India and Burma. *J. Meteor.*, **6**, 393–400.
Yoshimura, M., 1967: Annual change in the frontal zones in the Northern Hemisphere (in Japanese with English abstract). *Geograph. Rev. Japan*, **40**, 393–408.
Yoshino, M.M., 1965: Four stages of rainy season in early summer over East Asia (Part I). *J. Meteor. Soc. Japan*, **43**, 231–245.
Yoshino, M.M., 1966: Same as above (Part II). *J. Meteor. Soc. Japan*, **44**, 209–217.
Yoshino, M.M. and S. Yamakawa, 1985: Pressure pattern calendar of East Asia, 1971–1980, and some climatological discussions. *Climatological Notes*, **34**, pp 37.
Yu, D.R., 1980: The divisions of area Mei-yu season and single station Meu-yu period (in Chinese). *Meteor. Mon.*, 1980 (No. 10), 12–13.

1979年5月初め頃の日本南岸における準定常的梅雨前線の形成について

加藤内蔵進
(名古屋大学水圏科学研究所)
児玉安正
(弘前大学理学部地球科学科)

1979年5月初めにみられた日本南岸の準定常的梅雨前線の形成と、それに関係した東アジア大規模場の傾圧性の季節遷移について、観測資料に基づき議論する。

チベット高原南回りジェットに対応する日本南岸の前線帯は、4月には移動性高低気圧の通り道としての特徴をもつ。一方、5月になると、30°N付近を総観規模（あるいは大きいメソの規模）の低気圧の通過後でも、停滞前線に対応する雲帯が25°N付近に維持されやすい。言い換えれば、平均雲量極大ゾーンあるいは平均場の相当温位極大ゾーンとして定義される日本南岸の前線帯は、準定常的な性質を持つようになる（日本付近での準定常的な梅雨前線の形成）。1979年及び1985～1988年の1日2回の地上天気図上の前線の位置の解析により、5月の地上前線は準定常的な前線として出現しやすい事が、他の年についても示された。

5月になると、チベット高原を南北に回るジェットに対応する2つの傾圧帯が日本付近では分離し、日本付近の梅雨前線帯付近及びそのすぐ北側の傾圧性が弱まる。このため5月には傾圧不安定波としての移動性高気圧が発達しにくくなり、それにより前線帯の雲帯が壊されにくくなる事を通じて、準定常的な梅雨前線の維持に好都合な条件が与えられる。

Kato (1985, 1987a) は1979年5月後半に起きた大陸上の梅雨前線付近の南北温度傾度の急消失を指摘したが、本研究で示された5月初めの“準定常的”前線帯の形成は、季節進行の中で起きるそれとは別のイヴェントとして認識される。